Available online at www.sciencedirect.com

ScienceDirect

MATTER AND RADIATION AT EXTREMES

Matter and Radiation at Extremes 3 (2018) 40–49

www.journals.elsevier.com/matter-and-radiation-at-extremes

Research Article

Relaxation of non-isothermal hot dense plasma parameters

S.K. Kodanova [a,b], M.K. Issanova [a], S.M. Amirov [a,b], T.S. Ramazanov [a], A. Tikhonov [c], Zh.A. Moldabekov [a,b,*]

[a] *Institute for Experimental and Theoretical Physics, Al-Farabi Kazakh National University, 71 Al-Farabi Str., 050040 Almaty, Kazakhstan*
[b] *Institute of Applied Sciences and IT, 40-48 Shashkin Str., 050038 Almaty, Kazakhstan*
[c] *Nazarbayev University, Kabanbay Batyr Ave. 53, Astana 010000, Kazakhstan*

Received 13 May 2017; revised 14 July 2017; accepted 16 July 2017
Available online 6 September 2017

Abstract

The relaxation of temperature, coupling parameters, the excess part of equation of state, and the correlation energy of the non-isothermal hot dense plasmas are considered on the basis of the method of effective interaction potentials. The electron–ion effective interaction potential for the hot dense plasma is discussed. The accuracy of description of the dense plasma properties by the effective electron–ion interaction potential is demonstrated by the agreement of the derived quantities like stopping power and transport coefficients calculated using our methodology with the results of the finite-temperature Kohn-Sham density-functional theory molecular dynamics, and orbital-free molecular dynamics results as well as with the data obtained using other theoretical approaches.

PACS codes: 52.65.−y; 52.25.Dg; 52.27.Gr; 52.25.Kn

Keywords: Dense plasma; Effective potentials; Temperature relaxation; Stopping power; Transport

1. Introduction

The dense plasma is a subject of active experimental and theoretical investigations due to its importance to the inertial confinement fusion. The dense plasma forms in the experiments on heavy ion driven fusion [1–3], experiments at the National Ignition Facility [4], and magnetized Z-pinch experiments at Sandia [5]. To obtain a thermonuclear reaction in the above-mentioned facilities the comprehensive study of transport properties and relaxation times of the temperature of dense plasma is required. During compression of a target by the flow of high-energy particles the non-isothermal plasma with different temperatures of electrons and ions is created. Therefore, it is especially important to study relaxation times of electrons and ions. The temperature equalizes much faster within electronic and ionic subsystems than between electrons and ions. This is due to a large difference between masses of an ion and an electron. Computer simulation can answer many questions and, therefore, became the main theoretical method.

Programs for simulation and calculation of inertial confinement fusion targets are extremely complex and need a lot of computation time. The complexity of calculations is caused by a large number of different physical processes: temperature relaxation; change of thermodynamic properties; energy absorption; stopping power etc. In fact the description of one or more of these processes is already quite complicated.

One of the methods which allows fast calculation of the physical properties of isothermal plasmas is the method of effective interaction potentials. The method of effective interaction potentials [8–30] can provide possibility of fast and accurate calculations of temperature relaxation time, stopping power, and transport coefficients of dense plasmas.

* Corresponding author. Institute for Experimental and Theoretical Physics, Al-Farabi Kazakh National University, 71 Al-Farabi Str., 050040 Almaty, Kazakhstan.
E-mail address: zhandos@physics.kz (Zh.A. Moldabekov).
Peer review under responsibility of Science and Technology Information Center, China Academy of Engineering Physics.

http://dx.doi.org/10.1016/j.mre.2017.07.005

In this approach the screening (collective) and quantum diffraction effects are absorbed into an effective screened potential Φ:

$$\Phi_{\alpha\beta}(\boldsymbol{r}) = \int \frac{\mathrm{d}^3k}{2\pi^2} \frac{\phi_{\alpha\beta}(r)}{\epsilon(\boldsymbol{k},\omega)} \mathrm{e}^{\mathrm{i}\boldsymbol{k}\cdot\boldsymbol{r}}, \tag{1}$$

where $\phi_{\alpha\beta}(r)$ is the pair interaction potential, and $\epsilon(\boldsymbol{k},\omega)$ is the dielectric function. Further, we consider the static case $\omega = 0$.

The simplest model describing screened point-like charge potential is a Yukawa potential:

$$\Phi_{\mathrm{Y}}(r;n,T) = \frac{Q_1Q_2}{r}\mathrm{e}^{-k_{\mathrm{Y}}r}, \tag{2}$$

with the familiar inverse Yukawa screening length, k_{Y}.

Yukawa potential (2) can be derived using Thomas-Fermi model [25], or long wavelength limit of the polarization (response) function in random phase approximation (RPA). Recently screened ion potential taking into account the Kirzhnits first order gradient correction to the noninteracting free energy density functional was obtained by Akbari-Moghanjoughi [26] for zero temperature limit on the basis of the quantum hydrodynamic theory and at the finite temperature by Stanton and Murillo (SM) in the framework of the orbital-free density functional theory (OFDFT) [25].

Analysis of the available analytical formulas for the screened ion potential has been performed by Moldabekov et al. [27]. In Refs [9,16,25–27,32–34], the ion potential (ion–ion interaction potential) in the static limit which takes into account quantum non-locality (diffraction) effect caused by electrons was considered. Dynamically screened potentials in classical, quantum as well as relativistic systems were analyzed in Refs [17,35–40].

In this paper we present results for stopping power, transport coefficients, and temperature relaxation obtained using the effective interaction potential between electrons and ions in dense plasmas. The effective potential is derived using the long wavelength expansion of the polarization function and quantum potential which takes into account the finite value of the interaction potential at close distance.

In Sec. 2 the effective potential of electron–ion interaction is discussed. In Secs. 3 and 4 we present the results of calculation of the stopping power and transport properties of the dense isothermal plasma, respectively. In these sections comparisons with the results of other theoretical approaches (methods) are given. In Sec. 5 the temperature relaxation and related evaluation of the thermodynamical properties are presented.

2. Effective electron–ion interaction potential

The dielectric function in the RPA reads

$$\epsilon(\boldsymbol{k},0) = 1 - \frac{4\pi e^2}{k^2}\Pi_{\mathrm{RPA}}(k) - \frac{4\pi Z^2e^2}{k^2}\Pi_{\mathrm{ion}}(k). \tag{3}$$

where $\Pi_{\mathrm{ion}}(k)$ is the polarization function of ions, and $\Pi_{\mathrm{RPA}}(k)$ is the polarization function of quantum electrons at finite temperature [41]:

$$\Pi_{\mathrm{RPA}}(k,\omega) = -\frac{k^2\chi_0^2}{16\pi e^2 z^3}[g_3(u+z) - g_3(u-z)], \tag{4}$$

where $u = \omega/(kv_{\mathrm{F}})$, $z = k/(2k_{\mathrm{F}})$, $\chi_0^2 = 3/16\left(\hbar\omega_{\mathrm{p}}/E_{\mathrm{F}}\right)^2 = 1/(\pi k_{\mathrm{F}}a_{\mathrm{B}})$, $k_{\mathrm{F}} = (3\pi^2n_{\mathrm{e}})^{1/3}$, $\omega_{\mathrm{p}}^2 = 4\pi n_{\mathrm{e}}e^2/m_{\mathrm{e}}$, $a_{\mathrm{B}} = \hbar^2/m_{\mathrm{e}}e^2$ is the Bohr radius, v_{F} is Fermi velocity, and

$$g_3(x) = -g_3(-x) = \int \frac{y\,\mathrm{d}y}{\exp(y^2/\theta - \eta) + 1} \ln\left|\frac{x+y}{x-y}\right|, \tag{5}$$

where $\theta = k_{\mathrm{B}}T/E_{\mathrm{F}}$ is the degeneracy parameter, $\eta = \mu/k_{\mathrm{B}}T$ is the chemical potential which depends on the density via relation $2/3\theta^{-3/2} = I_{1/2}(\eta)$, and I_ν is the Fermi integral of order ν.

In Ref. [27] the following formula for the wavenumber expansion of the inverse polarization function was presented:

$$\frac{1}{2\Pi(\boldsymbol{k})} = \tilde{a}_0 + \tilde{a}_2\boldsymbol{k}^2 + \tilde{a}_4\boldsymbol{k}^4 + \ldots \tag{6}$$

Substituting the second order result of equation (6) into (3) and using long wavelength limit of the ions' classical polarization function $\Pi_{\mathrm{ion}}(\boldsymbol{k}) = -n_{\mathrm{i}}/(k_{\mathrm{B}}T_{\mathrm{i}})$, we have:

$$\epsilon_2(\boldsymbol{k})^{-1} = \frac{k^2\left(1 + \frac{\tilde{a}_2}{\tilde{a}_0}k^2\right)}{k^2\left(1 + \frac{\tilde{a}_2}{\tilde{a}_0}k_{\mathrm{i}}^2\right) + k_{\mathrm{D}}^2 + \frac{\tilde{a}_2}{\tilde{a}_0}k^4}, \tag{7}$$

where $k_{\mathrm{D}}^2 = \lambda_{\mathrm{D}}^{-2} = k_{\mathrm{Y}}^2 + k_{\mathrm{i}}^2$, $k_{\mathrm{i}}^2 = 4\pi n_{\mathrm{i}}Z_{\mathrm{i}}^2e^2/k_{\mathrm{B}}T_{\mathrm{i}}$, and $k_{\mathrm{Y}}^2 = k_{\mathrm{TF}}^2\theta^{1/2}I_{-1/2}(\eta)/2$ is the inverse screening length which interpolates between Debye and Thomas-Fermi expansions.

The result for $\tilde{a}_2/\tilde{a}_0$ is

$$\frac{\tilde{a}_2}{\tilde{a}_0} = \frac{I_{-3/2}(\eta)}{12\theta k_{\mathrm{F}}^2 I_{-1/2}^2(\eta)}. \tag{8}$$

Further the electrons density is characterized by the density parameter $r_{\mathrm{S}} = a/a_{\mathrm{B}}$, where $a = (4/3\pi n_{\mathrm{e}})^{-1/3}$.

In Ref. [9], a similar inverse dielectric function was obtained on the basis of the classical polarization function of electrons $\Pi(\boldsymbol{k}) = -n_{\mathrm{e}}/(k_{\mathrm{B}}T_{\mathrm{e}})$, but using the quantum Deutsch [42] potential for the electron–electron interaction $\phi_{\mathrm{ee}}^{\mathrm{Deutsch}} = e^2/r[1 - \exp(-r/\lambda_{\mathrm{ee}})]$ instead of the Coulomb interaction. However, Eq. (7) is preferable as it was derived directly from the fully quantum polarization function in the RPA.

We neglect the bound state effect and use the Deutsch quantum potential [42]:

$$\phi_{\mathrm{ei}} = \frac{Ze^2}{r}[1 - \exp(-r/\lambda_{\mathrm{ei}})], \tag{9}$$

which has the finite value at $r \to 0$:

$$\lim_{r\to 0}\phi(r) = \frac{Ze^2}{\lambda_{\mathrm{ei}}}, \tag{10}$$

where $\lambda_{\mathrm{ei}} = \hbar/\sqrt{\pi m_{\mathrm{ei}}k_{\mathrm{B}}T_{\mathrm{ei}}}$ is the thermal wavelength characterizing the manifestation of the electron wave nature in the

pair interaction potential, m_{ei} is the reduced mass of the considered pair of particles, and Z is the ion charge number.

In order to describe the nonisothermal two-temperature plasma not only temperatures of electrons and ions but also the electron–ion temperature T_{ei} is required [43,44]. Using the Ornstein–Zernike equation, it was suggested that the electron–ion temperature should be expressed in terms of electron and ion temperatures as following [44]:

$$T_{ei} = \sqrt{T_e T_i}. \tag{11}$$

Substituting Eq. (7) into Eq. (1), for the electron–ion effective interaction potential Φ_{ei} we find:

$$\Phi_{ei}(r) = -\frac{Ze^2}{r\lambda_{ee}^2\gamma^2\sqrt{1-\left(2k_D/\lambda_{ee}\gamma^2\right)^2}}\left[\left(\frac{1-\lambda_{ee}^2B^2}{1-\lambda_{ei}^2B^2}\right)\exp(-rB) - \left(\frac{1-\lambda_{ee}^2A^2}{1-\lambda_{ei}^2A^2}\right)\exp(-rA)\right] + \frac{Ze^2\exp(-r/\lambda_{ei})}{r(1+C_{ei})}, \tag{12}$$

where $A^2 = \gamma^2/2[1+\sqrt{1-(2k_D/\lambda_{ee}\gamma^2)^2}\,]$, $B^2 = \gamma^2/2[1-\sqrt{1-(2k_D/\lambda_{ee}\gamma^2)^2}\,]$, $C_{ei} = \left(k_D^2\lambda_{ei}^2 - k_i^2\lambda_{ee}^2\right)/\left(\lambda_{ee}^2/\lambda_{ei}^2 - 1\right)$, $\gamma^2 = k_i^2 + 1/\lambda_{ee}^2$, $\lambda_{ee}^2 = -b_1/4k_F^2$ (here $b_1 = \theta^{-1}I_{-3/2}(\eta)/\left[3I_{-1/2}^2(\eta)\right]$).

The electron–ion effective interaction potential (12) has the same form as the screened potential in Ref. [9] which obtained on the basis of a semi-classical dielectric function. Potential (12) differs from the screened potential of Ref. [9] in definition of the coefficient λ_{ee} as the fully quantum expression for the polarization function is used.

If the electron is considered as a point-like charged particle $\lambda_{ei} \to 0$, potential (12) agrees with the SM potential [25] (note that the SM potential is for the ion–ion interaction). If the quantum non-locality is neglected $\lambda_{ee} \to 0$, potential (12) reproduces the Yukawa (Debye) potential (2) with $Q_1Q_2 = -Ze^2$.

Recently, analyzing Baimbetov's method of pseudo potentials W. Ebeling suggested using $\lambda_{Eb} = \hbar\sqrt{\pi}/(4\sqrt{m_{ei}k_BT_{ei}})$ as the parameter characterizing the thermal wavelength in the Deutsch potential [45]. This choice results in the exact reproduction of the first quantum corrections to classical thermodynamics and improvements of the overall plasma thermodynamics for the higher orders. However, better performance in the description of the thermodynamical properties does not guarantee better description of the dynamical properties such as stopping power and transport coefficients. In fact, the Deutsch choice of the λ_{ei}, which hereafter is referred explicitly as λ_{De}, is appears to provide a rather better description of the mentioned dynamical properties as it is demonstrated below.

3. Stopping power

One of the most important characteristics which describes the interaction of ions with matter is the stopping power (see e.g. Ref. [47] and references therein). The stopping power describes the rate of loss of the kinetic energy of directed motion of a projectile in matter.

We calculate the stopping power in the binary collision approximation [12,13]:

$$\frac{dE}{dx} = 8\pi n\left(\frac{m_{ei}}{m_i}\right)\cdot E_c\cdot\rho_\perp^2\cdot\Lambda_{ei}, \tag{13}$$

here $E_c = 1/2m_{ei}v^2$ is the energy of the center of mass of the colliding particles, m_{ei} is the reduced mass of ions or electrons, v is the relative velocity of the scattered test particle, $\rho_\perp = Ze^2/2E_c$, and Λ_{ei} is the Coulomb logarithm.

The Coulomb logarithm is determined by the scattering angle [46]:

$$\Lambda_{ei} = \frac{1}{\rho_\perp^2}\int_0^\infty \sin^2\left[\frac{\chi(\rho)}{2}\right]\rho\, d\rho. \tag{14}$$

The classical scattering angle for two particles with masses m_1, m_2 and with the interparticle interaction potential $\Phi_{ei}(r)$ for a given impact parameter ρ reads

$$\chi(\rho) = |\pi - 2\varphi(\rho)|, \tag{15}$$

where

$$\varphi(\rho) = \rho\int_{r_{min}}^\infty \frac{dr}{r^2\sqrt{1-U_{eff}(r,\rho)}}, \tag{16}$$

and U_{eff} is the effective interaction energy taking into account centrifugal force due to momentum conservation law has the following form

$$U_{eff}(r,\rho) = \frac{\rho^2}{r^2} + \frac{2\Phi_{ei}(r)}{mv^2}, \tag{17}$$

where U_{eff} is given in the units of kinetic energy of the projectile.

In Eq. (16), r_{min} is the distance of the closest approach at the given impact parameter. $\chi(\rho)$ is obtained from the equation $U_{eff}(r_{min},\rho) = 1$.

The effect of dynamic screening is taken into account by the following expression, which was recently suggested on the basis of highly accurate molecular dynamics data obtained by Grabowski et al. [48]. Consequently, the screening length was rescaled as

$$\lambda_D^* \to \lambda_D \sqrt{1+(v/v_{th})^2\left(1+\Gamma^3\right)^{1/4}}, \tag{18}$$

here $v_{th}=\sqrt{k_B T/m_e}$, and $\Gamma = e^2/ak_B T$ is the plasma non-ideality parameter.

Hereafter, the effective electron–ion interaction potential with the rescaled screening length λ_D^* will be referred to as the dynamic screened potential.

More accurately, to include the dynamic screening effects in the weakly non-ideal plasma the following scheme suggested by Gould and DeWitt can be used [49,60]:

$$\frac{\partial\langle E\rangle}{\partial x} = \frac{\partial\langle E\rangle^{\text{static}}_{\text{T matrix}}}{\partial x} + \frac{\partial\langle E\rangle^{\text{dynamic}}_{\text{Born}}}{\partial x} - \frac{\partial\langle E\rangle^{\text{static}}_{\text{Born}}}{\partial x}. \tag{19}$$

Further, the ansatz (19) is referred to as a combined model. In the combined model the stopping power is calculated as the sum of the T-matrix and the dynamic random phase approximation (RPA) subtracting the static first Born term to avoid double counting. The main idea of the combined approach is inclusion of the dynamic screening in the RPA taking into account strong coupling (non-ideality) by the T-matrix method.

The quality of the description of the dynamic properties on the basis of the effective potential (12) is checked by the comparison of the stopping power calculated using the combined model, *T*-matrix method and the first order Born approximation with the data obtained using the effective electron–ion potential (12).

The stopping power obtained using the effective potential (12) and the results of calculations using the combined model, the first Born approximation, *T*-matrix model, dynamic RPA, and particle in cell (PIC) simulation are shown in Figs. 1–3. Without rescaling of the screening length the effective potential (12) correctly describes the stopping power at $v \lesssim v_{th}$. Rescaling of the screening length extends the applicability range of the potential (12) up to $v \lesssim 1.5\ v_{th}$. The data obtained from the combined model have a agreement with the simulation data at velocities $v \lesssim 3\ v_{th}$. In cases $Z=5$ and $Z=10$, at high velocities the effective potential (12) gives the results closer to the Born approximation. Additionally, from Figs. 1–3 it can be concluded that the thermal wavelength proposed by Ebeling fails to provide correct description of the stopping power.

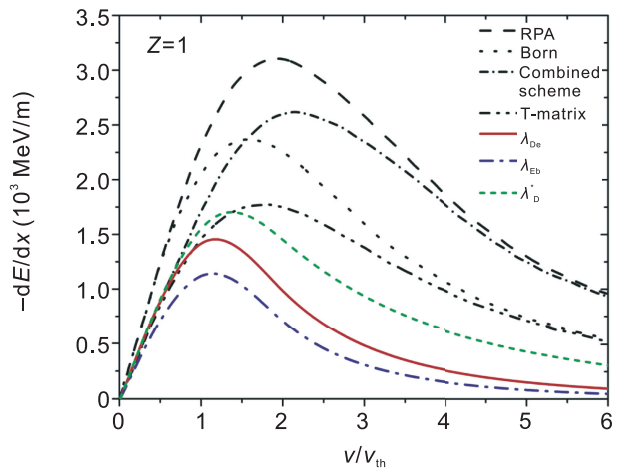

Fig. 1. Stopping power obtained on the basis of the effective interaction potential (12) with and without rescaling of the screening length in comparison with the results of different theoretical approaches [60] for $Z=1$. Data calculated using the Deutsch thermal wavelength are denoted as λ_{De}. The results obtained using the thermal wavelength proposed by Ebeling are denoted as λ_{Eb}. The result obtained taking into account the dynamic screening by rescaling the screening length is denoted as λ_D^*.

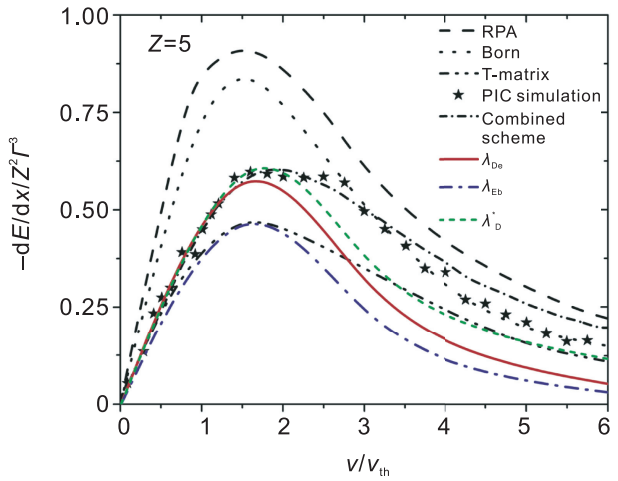

Fig. 2. Stopping power obtained on the basis of the effective interaction potential (12) with and without rescaling of the screening length in comparison with the results of different theoretical approaches [60] for $Z=5$. Data calculated using the Deutsch thermal wavelength are denoted as λ_{De}. The results obtained using the thermal wavelength proposed by Ebeling are denoted as λ_{Eb}. The result obtained taking into account the dynamic screening by rescaling the screening length is denoted as λ_D^*. The stopping power is given in units of $3k_B T/\lambda_D$.

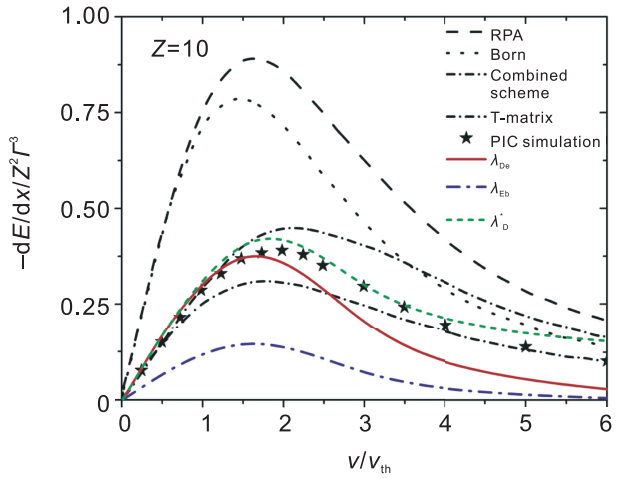

Fig. 3. Stopping power obtained on the basis of the effective interaction potential (12) with and without rescaling of the screening length in comparison with the results of different theoretical approaches [60] for $Z=10$. Data calculated using the Deutsch thermal wavelength are denoted as λ_{De}. The results obtained using the thermal wavelength proposed by Ebeling are denoted as λ_{Eb}. The result obtained taking into account the dynamic screening by rescaling the screening length is denoted as λ_D^*. The stopping power is given in units of $3k_B T/\lambda_D$.

4. Transport properties

Investigation of transport properties is important for ICF, physics of warm dense matter, etc. [51]. In particular, realization of the inertial confinement fusion requires reliable information about transport coefficients, i.e. coefficients of thermal conductivity, and diffusion. We consider the dense DT plasma.

The plasma diffusion coefficient, and thermal conductivity are connected with the effective collision frequency:

$$D = \frac{k_B T}{m_e \nu_{eff}}, \tag{20}$$

$$k = \frac{5 n_e k_B^2 T}{m_e \nu_{eff}}, \tag{21}$$

where

$$\nu_{eff} = (4/3)\sqrt{2\pi} e^4 \Lambda_{ei} / \sqrt{m_e} (k_B T)^{3/2} \tag{22}$$

is the effective collision frequency determining by the Coulomb logarithm. The dimensionless diffusion and thermal conductivity coefficients are $D^* = D/\omega_p a^2$, and $k^* = k/(m_e \omega_p / a)$, respectively (here $\omega_p = (4\pi n_i/M)^{1/2} Ze$ is the plasma frequency for ions mass M). For the DT mixture considered in this work we use $M = (2+3)/2 = 2.5$ amu [52].

In Figs. 4 and 5 the results for thermal conductivity of the dense plasma as a function of temperature are presented. The red solid lines represent the thermal conductivity obtained using the effective interaction potential (12), the blue solid lines are the result obtained using λ_{Eb} as a thermal wavelength. The black solid triangles represent the QMD results [53]. The blue dash-dotted lines represent the common Coulomb logarithm Λ:

$$\Lambda = \ln \frac{b_{max}}{b_{min}}, \tag{23}$$

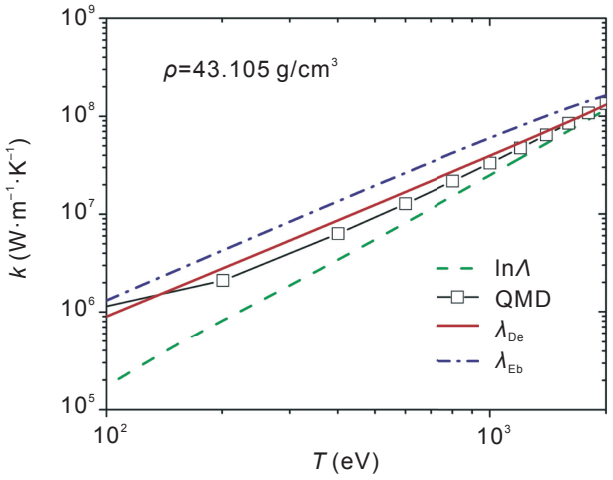

Fig. 4. Thermal conductivity of the DT plasma obtained using the effective interaction potential (12) and from QMD simulations as a function of temperature at $\rho = 43.105$ g/cm^3. The results obtained using the thermal wavelength proposed by Ebeling are denoted as λ_{Eb}.

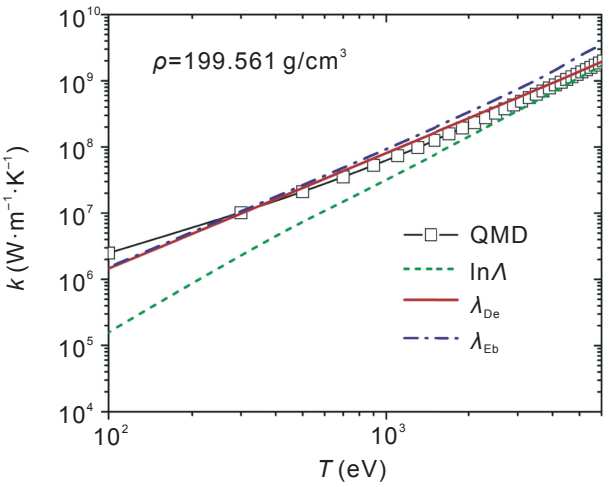

Fig. 5. Thermal conductivity of the DT plasma obtained using the effective interaction potential (12) and from QMD simulations as a function of temperature at $\rho = 199.561$ g/cm^3. The results obtained using the thermal wavelength proposed by Ebeling are denoted as λ_{Eb}.

where b_{max}, b_{min} are maximal and minimal impact parameters. As the minimal impact parameter the closest approach distance $Ze^2/k_B T$ or de Broglie thermal wavelength λ_{ei} is taken depending which of them has a larger value.

In [53] QMD simulations, the results for the deuterium thermal conductivity were provided for a wide range of densities and temperatures. Hu et al. [53] presented the following function to fit the results of the QMD calculations:

$$k_{QMD} = \frac{20(2/\pi)^{3/2} k_B^{7/2} T^{5/2}}{\sqrt{m_e} Z_{eff} e^4} \times \frac{0.095(Z_{eff} + 0.24)}{1 + 0.24 Z_{eff}} \frac{1}{\Lambda_{QMD}}, \tag{24}$$

From Figs. 4 and 5 one can see that the thermal conductivity of deuterium plasma increases as the temperature increases. Note that at high densities and relatively low temperatures the results obtained using the effective potential are close to the result obtained using quantum molecular dynamics.

We calculated the diffusion coefficient of the deuterium–tritium plasma for density $\rho = 5$ g/cm^3 and temperatures ranging from 2 to 10 eV using the Coulomb logarithm based on the effective potential (12). Fig. 6 shows a comparison of the calculated data on diffusion in a DT plasma with the theoretical results from Refs. [54–57]. The comparison with the data obtained on the basis of the finite-temperature Kohn-Sham density-functional theory molecular dynamics (QMD) and orbital-free molecular dynamics (OFMD) are given. OFMD simulations consider the free energy of electrons semiclassically, and are able to reach higher temperatures. The obtained results are in good agreement with the results of QMD and OFMD simulations at higher temperatures, and therefore we conclude that our method can be used in this regime. The reason for this is that the effective interaction potential using our calculations takes into account the first order gradient correction as it has been mentioned. At temperatures below 3 eV, the correlations (non-ideality) become important and the effective potential (12) does not

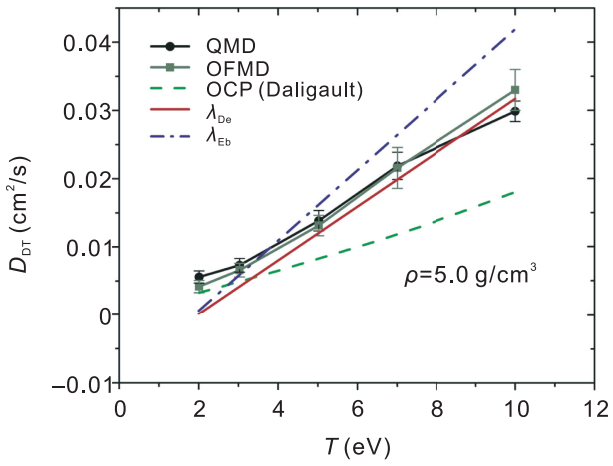

Fig. 6. The diffusion coefficient for the DT plasma a function of temperature at density $\rho = 5$ g/cm^3. The results obtained using the thermal wavelength proposed by Ebeling are denoted as λ_{Eb}. Comparisons with the results of QMD, OFMD [54], and OCP classical simulation [55] are given.

work as it was derived on the basis of the RPA. Additionally, from the presented data for the transport coefficients it is clear that the change of the thermal wavelength, $\lambda_{ei} \to \lambda_{Eb}$, to improve the description of the thermodynamic properties of the plasma leads to the incorrect description of the diffusion and thermal conductivity.

5. Temperature relaxation

The results on the stopping power and transport properties for the isothermal case show that the effective potential (12) provides correctly qualitative and quantitative description of hot dense plasmas. Assuming that this holds for the non-isothermal plasma, in this section temperature relaxation and related change in the thermodynamical properties are considered.

The relaxation rate of the electron–ion temperature (the rate of energy exchange) is determined by the difference of the average temperatures:

$$\frac{dT_e}{dt} = \frac{T_i - T_e}{\tau_{ei}}, \frac{dT_i}{dt} = \frac{T_e - T_i}{\tau_{ie}}, \tag{25}$$

$$\tau_{ei} = \frac{3m_e m_i}{8\sqrt{2\pi} n e^2 \Lambda_{ei}} \left(\frac{k_B T_e}{m_e} + \frac{k_B T_i}{m_i} \right)^{3/2}. \tag{26}$$

The relaxation times of the temperature in the plasma are calculated for different density values on the basis of the Coulomb logarithm using the effective potential (12). Fig. 7 shows the values of temperatures of ions and electrons at $n = 10^{24}$ cm^{-3} in comparison with MD data and the results of other theoretical methods. When the time given in the logarithm scale, the relaxation can be divided into two stages. The first one, at the beginning of the relaxation process, is characterized by the slow equilibration of temperatures. The second stage, at large times, is characterized by the exponential decrease of the temperature difference of components. In Figs. 8 and 9 the relaxation of the temperature at two different values of the initial ion temperature and plasma density are presented. The equilibration rate increases with increasing density, which is caused by the increase in the frequency of collisions. The larger the temperature difference between electrons and ions, the more time is needed to come to an equilibrium state. According to the data from Figs. 8 and 9, the change of the ion–ion coupling parameter $\Gamma_i = e^2/ak_B T_i$ and of the electron–electron coupling parameter $\Gamma_e = e^2/ak_B T_e$ are presented in Figs. 10 and 11. The ion–ion coupling parameter Γ_i decreases due to heating of the ions, whereas the electron–electron coupling parameter Γ_e increases due to cooling of the electrons.

Now it is interesting to consider the changes in the thermodynamical properties of the dense plasma in the course the temperature equilibration. For this reason, further it is assumed that the plasma is always in the local thermodynamic equilibrium state.

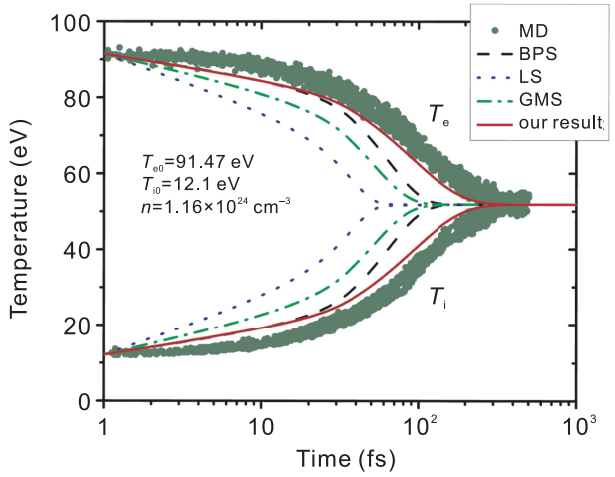

Fig. 7. Comparison of the values of temperature relaxation calculated on the basis of the effective potential with other theoretical BPS [58], LS [59], GMS [60] and MD results [61].

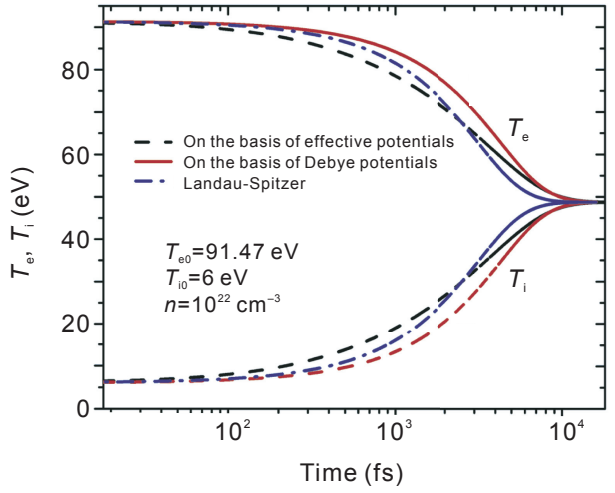

Fig. 8. The relaxation of temperature calculated on the basis of the effective potential, the Yukawa (Debye) potential, and using Landau-Spitzer theory at $n = 10^{22}$ cm^{-3}.

To study the thermodynamic properties of the plasma we used a method using particle pair correlation function in the following approximation:

$$g_{\alpha\beta}(r) \simeq 1 + \frac{\Phi_{\alpha\beta}(r)}{k_B T_{\alpha\beta}}, \tag{27}$$

where $T_{ee} = T_e$, $T_{ii} = T_i$ are the temperatures of the electron and ion subsystems, and $T_{ei} = T_{ie}$ is the electron–ion temperature (see Eq. (11)).

The approximation (27) is justified as in the considered cases the coupling (non-ideality) parameters have values less than one (see Figs. 10 and 11).

The correlation energy in terms of the pair correlation function reads:

$$U_N = 2\pi V \int \sum_{\alpha,\beta} n_\alpha n_\beta \phi_{\alpha\beta}(r) g_{\alpha\beta}(r) r^2 \mathrm{d}r. \tag{28}$$

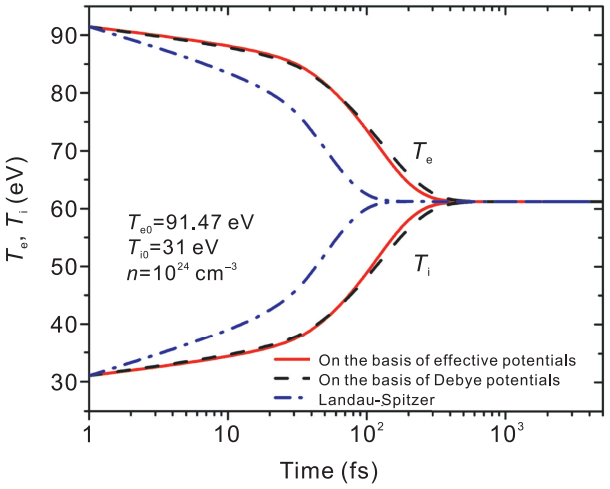

Fig. 9. The relaxation of temperature calculated on the basis of the effective potential, the Yukawa (Debye) potential, and using Landau-Spitzer theory at $n = 10^{24}$ cm^{-3}.

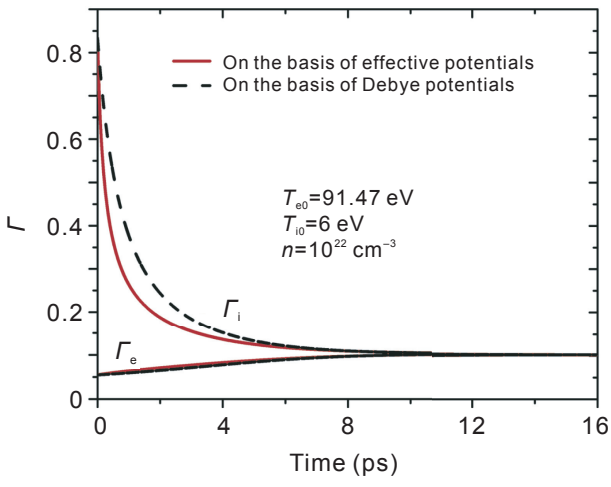

Fig. 10. The relaxation of the coupling (non-ideality) parameters Γ_e, and Γ_i at $n = 10^{22}$ cm^{-3}.

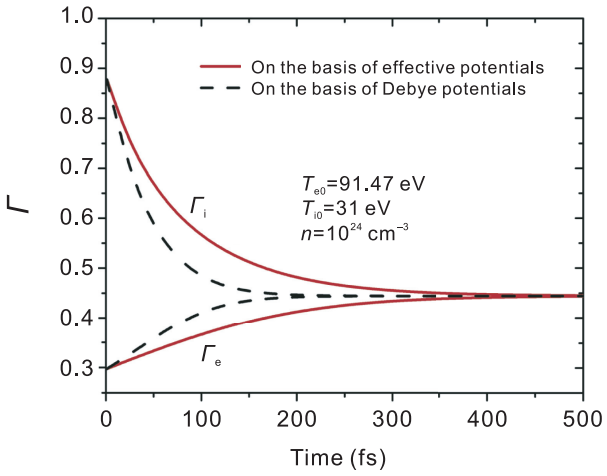

Fig. 11. Relaxation of the coupling (non-ideality) parameters Γ_e, and Γ_i at $n = 10^{24}$ cm^{-3}.

The plasma equation of state is determined by the equation:

$$P = P_{ideal} + \frac{2\pi}{3} \int \sum_{\alpha,\beta} n_\alpha n_\beta \frac{\mathrm{d}\phi_{\alpha\beta}(r)}{\mathrm{d}r} g_{\alpha\beta}(r) r^3 \mathrm{d}r, \tag{29}$$

where P_{ideal} is the pressure of ideal plasma. In this approximation, for the correlation energy it was obtained [9,62]:

$$U_N = -2\pi V \sum_{\alpha,\beta} \frac{n_\alpha n_\beta e_\alpha^2 e_\beta^2}{k_B T_{\alpha\beta} \gamma^2 \sqrt{1 - (2k_D/\lambda_{ee}\gamma^2)^2}} \times \left[\frac{1/\lambda_{ee}^2 - B^2}{B\left(1 - B^2\lambda_{\alpha\beta}^2\right)} - \frac{1/\lambda_{ee}^2 - A^2}{A\left(1 - A^2\lambda_{\alpha\beta}^2\right)} \right] + U_\lambda, \tag{30}$$

here the second term $U_\lambda = 2\pi V e^2 \{2Z_i n_i n_e \lambda_{ei}^2 - n_e^2 \lambda_{ee}^2 + Z_i n_i n_e \lambda_{ei} e^2/[k_B T_{ei}(1 + C_{ei})]\}$ is due to the quantum diffraction effect at small distances.

For the equation of state we found [9,62]:

$$P = P_{ideal} - \frac{2\pi}{3} \sum_{\alpha,\beta} \frac{n_\alpha n_\beta e_\alpha^2 e_\beta^2}{k_B T_{\alpha\beta} \gamma^2 \sqrt{1 - (2k_D/\lambda_{ee}\gamma^2)^2}} \times \left[\frac{1/\lambda_{ee}^2 - B^2}{B\left(1 - B^2\lambda_{\alpha\beta}^2\right)(1 + B\lambda_{\alpha\beta})^2} - \frac{1/\lambda_{ee}^2 - A^2}{A\left(1 - A^2\lambda_{\alpha\beta}^2\right)(1 + A\lambda_{\alpha\beta})^2} \right] + P_\lambda, \tag{31}$$

here the second term $P_\lambda = 2\pi e^2 \{2Z_i n_i n_e \lambda_{ei}^2 - n_e^2 \lambda_{ee}^2 + Z_i n_i n_e \lambda_{ei} e^2/[12 k_B T_{ei}(1 + C_{ei})]\}$.

Equations for the correlation energy (30) and for the equation of state (31) are consistent with the effective potential (12) used for the calculation of the temperature relaxation.

The relaxation of the correlation energy and the excess part of the equation of state at $n = 10^{22}$ cm^{-3} and at $n = 10^{24}$ cm^{-3} are presented in Figs. 12 and 13, respectively. In the case $n = 10^{22}$ cm^{-3} (with initial value of the ion

temperature 6 eV), at the first stage the heating of the ions leads to the decrease of the correlation energy and the excess part of the equation of state (by absolute values). In contrast, in the case $n = 10^{24}$ cm^{-3} (with initial value of the ion temperature 31 eV), cooling of electrons overcomes the effect of ionic heating and, therefore, the absolute values of both the correlation energy and the excess part of the equation of state increase. At the second stage, for both mentioned cases, stronger electron correlations caused by cooling of electrons leads to the increase in the correlation energy and the excess part of the equation of state (by absolute values).

In general, in the experiments on production of hot dense plasmas, initially the ionic subsystem can be heated first, i.e. $T_{i0} > T_{e0}$. For example, in the case when matter is compressed and heated by an ion beam. To provide a simplified analysis of both cases, i.e. $T_{i0} > T_{e0}$ and $T_{i0} < T_{e0}$, we present the correlation energy U_N and the excess part of the equation of state ΔP as a function of the electron–ion temperature ratio in Figs. 14 and 15. The data obtained neglecting the quantum non-locality effect inscreening of the inter-particle interaction (i.e. taking $\lambda_{ee} = 0$ in the dielectric function) and the results determined using the Yukawa (Debye) potential are given for the comparison. As it is seen from Figs. 14 and 15, the quantum non-locality leads to the weaker manifestation of the

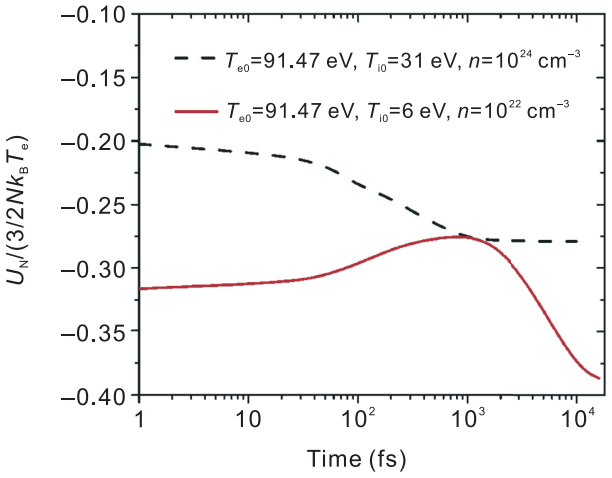

Fig. 12. Relaxation of the correlation energy of the non-isothermal hydrogen plasma. The values of temperatures of electrons and ions are given in Figs. 8 and 9. Corresponding relaxation of the coupling parameters is presented in Figs. 10 and 11. The values of the correlation energy in the case $n = 10^{22}$ cm^{-3} are multiplied by the factor 10.

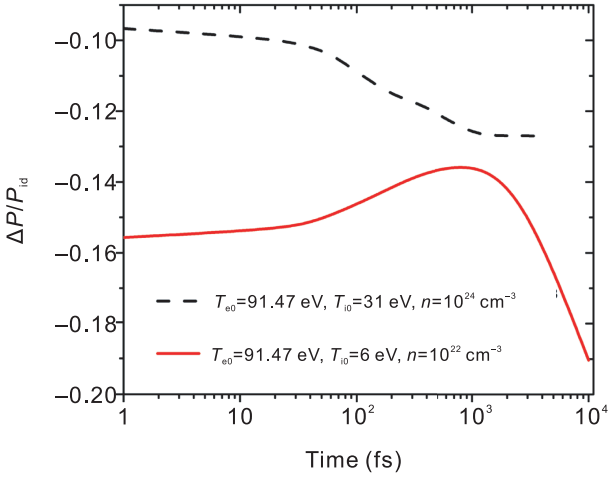

Fig. 13. Relaxation of the excess part of equation of state for the non-isothermal hydrogen plasma. The values of temperatures of electrons and ions are given in Figs. 8 and 9. Corresponding relaxation of the coupling parameters is presented in Figs. 10 and 11. The values of the excess part of equation of state in the case $n = 10^{22}$ cm^{-3} are multiplied by the factor 10.

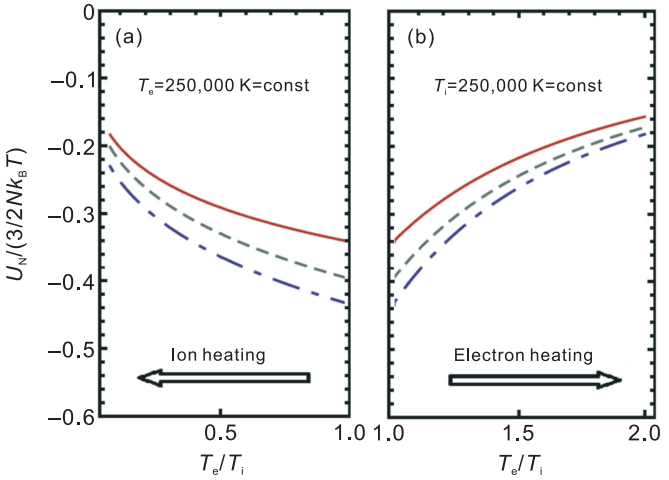

Fig. 14. Correlation energy of nonisothermal hydrogen plasma at (a) $T_e = 250,000$ K = const and (b) $T_i = 250,000$ K = const as a function of electron–ion temperature ratio T_e/T_i. The density parameter is $r_s = 3$. Solid line corresponds to Eq. (30), dashed line is obtained neglecting quantum non-locality effect in the plasma dielectric function (i.e. $\lambda_{ee} = 0$), dashed–dotted line presents the results of the Debye theory (i.e. $\lambda_{ee} = 0$ and $\lambda_{ei} = 0$).

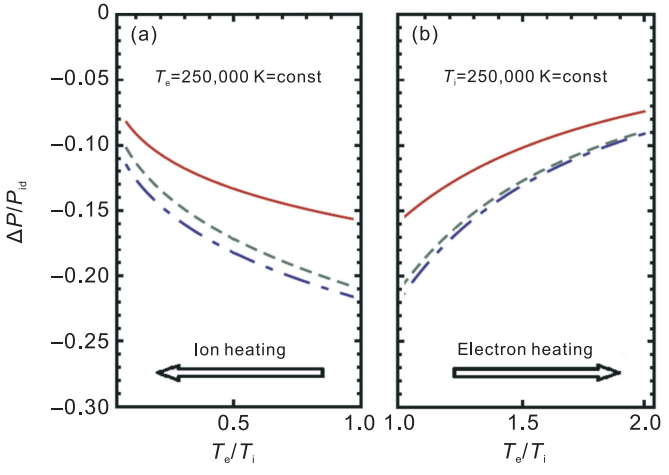

Fig. 15. The excess part of the equation of state for the non-isothermal hydrogen plasma at (a) $T_e = 250,000$ K = const and (b) $T_i = 250,000$ K = const as a function of electron–ion temperature ratio T_e/T_i. The density parameter is $r_s = 3$. Solid line corresponds to Eq. (31), dashed line obtained neglecting the quantum non-locality effect in the plasma dielectric function (i.e. $\lambda_{ee} = 0$), dashed-dotted line presents the results of the Debye theory (i.e. $\lambda_{ee} = 0$ and $\lambda_{ei} = 0$).

non-ideality in two-component plasma thermodynamics. Heating of ions (or electrons) leads to the decrease in the absolute values of U_N and ΔP, whereas cooling of ions (or electrons) gives the opposite result. During relaxation of temperatures of electrons and ions, the hotter component undergoes cooling while the cooler component heats up until the equilibration of temperatures.

6. Conclusions

In this work the temperature relaxation and related relaxation of the thermodynamical properties of the hot dense plasma are considered on the basis of the effective interaction potential. The applicability of the proposed effective electron−ion interaction potential is justified by the agreement of the calculated data on the stopping power and transport coefficients with the results of such computer simulations as PIC, QMD, OFMD and other theoretical methods.

It is shown that the modification of the thermal wavelength in the Deutsch potential (9) proposed in Ref. [45] for better description of thermodynamical properties does not result in improved description of such dynamical properties as stopping power, thermal conductivity, and the diffusion coefficient of plasmas.

Assuming that the condition of the local thermodynamic equilibrium is satisfied, the relaxation of the coupling parameters, the correlation energy, and the excess part of equation of state of the nonisothermal hot dense plasma are obtained. Depending on the difference in the initial values of the temperatures of electrons and ions, thermodynamical properties can undergo non-monotonic changes in the course of relaxation to equilibrium. However, first of all, we neglected possible impact of the ion−electron recombination at $r_s > 2$. The second point is that the question of the choice of electron−ion temperature T_{ei} is still open. This parameter is critical for the description of the non-isothermal plasma in the framework of theoretical methods.

Finally, the third important issue related to the extension of the method to non-ideal dense quantum plasmas, is the consistent inclusion of the effect of non-ideality into the pair interaction potential between particles taking into account such collective effects as the ionization energy depression (reduction) and exchange-correlation effects.

The development of the method of effective interaction potentials is important as it gives a deeper insight into physics of dense plasmas [63] and can provide an effective tool for the fast and accurate calculation of various physical properties for future technological applications [64]. Therefore, the above-mentioned issues need to be addressed in future works.

Acknowledgments

This research was funded under the program number 011503029 NU-Berkeley strategic initiative in warm-dense matter, advanced materials and energy sources for 2014−2018 and under Grant No. 0263/PSF from the Ministry of Education and Science of the Republic of Kazakhstan.

Conflict of interest

The authors declare that there is no conflicts of interest.

References

[1] D.H.H. Hoffmann, A. Blazevic, O. Rosmej, M. Roth, N.A. Tahir, et al., Present and future perspectives for high energy density physics with intense heavy ion and laser beams, Laser Part. Beams 23 (2005) 47−53.
[2] B. Yu. Sharkov, D.H.H. Hoffmann, A.A. Golubev, Y. Zhao, High energy density physics with intense ion beams, Matter Radiat. Extrem. 1 (2016) 28−47.
[3] S. Kawata, T. Karino, A.I. Ogoyski, Review of heavy-ion inertial fusion physics, Matter Radiat. Extrem. 1 (2016) 89−113.
[4] O.A. Hurricane, D.A. Callahan, D.T. Casey, P.M. Celliers, C. Cerjan, et al., Fuel gain exceeding unity in an inertially confined fusion implosion, Nature 506 (2014) 343.
[5] M.R. Gomez, S.A. Slutz, A.B. Sefkow, D.B. Sinars, K.D. Hahn, et al., Experimental demonstration of fusion-relevant conditions in magnetized liner inertial fusion, Phys. Rev. Lett. 113 (2014) 155003. P.F. Schmit, et al, Understanding Fuel Magnetization and Mix Using Secondary Nuclear Reactions in Magneto-Inertial Fusion, Phys. Rev. Lett. 113 (2014) 155004.
[8] M.K. Issanova, S.K. Kodanova, T.S. Ramazanov, D.H.H. Hoffmann, Transport properties of inertial confinement fusion dense plasmas, Contrib. Plasma Phys. 56 (5) (2016) 425.
[9] T.S. Ramazanov, Zh.A. Moldabekov, M.T. Gabdullin, Effective potentials of interactions and thermodynamic properties of a nonideal two-temperature dense plasma, Phys. Rev. E 92 (2015) 023104.
[10] T. Ramazanov, Zh. Moldabekov, M. Gabdullin, Multipole expansion in plasmas: effective interaction potentials between compound particles, Phys. Rev. E 93 (2016) 053204.
[11] T.S. Ramazanov, Zh.A. Moldabekov, M.T. Gabdullin, T.N. Ismagambetova, Interaction potentials and thermodynamic properties of two component semiclassical plasma, Phys. Plasmas 21 (2014) 012706.
[12] C.A. Ordonez, M.I. Molina, Evaluation of the Coulomb logarithm using cutoff and screened Coulomb potentials, Phys. Plasmas 1 (1994) 2515.
[13] T.S. Ramazanov, S.K. Kodanova, Coulomb logarithm of a nonideal plasma, Phys. Plasmas 8 (2001) 5049.
[14] S.K. Kodanova, T.S. Ramazanov, M.K. Issanova, G.N. Nigmetova, Zh.A. Moldabekov, Investigation of Coulomb logarithm and relaxation processes in dense plasma on the basis of effective potentials, Contrib. Plasma Phys. 55 (2015) 271.
[15] M.K. Issanova, S.K. Kodanova, T.S. Ramazanov, N.Kh. Bastykova, Zh.A. Moldabekov, et al., Classical scattering and stopping power in dense plasmas: the effect of diffraction and dynamic screening, Laser Part. Beams 34 (2016) 457−466.
[16] T.S. Ramazanov, S.K. Kodanova, Zh.A. Moldabekov, M.K. Issanova, Dynamical properties of non-ideal plasma on the basis of effective potentials, Phys. Plasmas 20 (2013) 112702.
[17] Zh.A. Moldabekov, P. Ludwig, J.P. Joost, M. Bonitz, T.S. Ramazanov, Dynamical screening and wake effects in classical, quantum, and ultra-relativistic plasmas, Contrib. Plasma Phys. 55 (2015) 186.
[18] Zh.A. Moldabekov, P. Ludwig, M. Bonitz, T.S. Ramazanov, Notes on anomalous quantum wake effects, Contrib. Plasma Phys. 56 (2016) 442.
[19] T.S. Ramazanov, K.N. Dzhumagulova, A.Zh. Akbarov, Cross sections and transport coefficients of dense partially ionized semiclassical plasma, J. Phys. A Math. Gen. 39 (2006) 4335.
[20] M.-Y. Song, Y.-D. Jung, Quantum screening effects on the electron-ion occurrence scattering time advance in strongly coupled semiclassical plasmas, Phys. Plasmas 10 (2003) 3051.
[21] H.-M. Kim, Y.-D. Jung, Quantum effects on polarization transport scatterings in partially ionized dense hydrogen plasmas, Phys. Plasmas 14 (2007) 074501.
[22] D.-H. Ki, Y.-D. Jung, Quantum screening effects on the ion-ion collisions in strongly coupled semiclassical plasmas, Phys. Plasmas 17 (2010) 074506.

[23] F.B. Baimbetov, Kh.T. Nurekenov, T.S. Ramazanov, Pseudopotential theory of classical non-ideal plasmas, Phys. Lett. A 202 (1995) 211.
[24] F.B. Baimbetov, Kh.T. Nurekenov, T.S. Ramazanov, Electrical conductivity and scattering sections of strongly coupled hydrogen plasmas, Phys. A 226 (1996) 181.
[25] L.G. Stanton, M.S. Murillo, Unified description of linear screening in dense plasmas, Phys. Rev. E 91 (2015) 033104. Pulisher's Note ibid: 91 (2015) 049901.
[26] M. Akbari-Moghanjoughi, Hydrodynamic limit of Wigner-Poisson kinetic theory: revisited, Phys. Plasmas 22 (2015) 022103. Erratum ibid: 22 (2015) 039904.
[27] Zh. Moldabekov, T. Schoof, P. Ludwig, M. Bonitz, T. Ramazanov, Statically screened ion potential and Bohm potential in a quantum plasma, Phys. Plasmas 22 (2015) 102104.
[28] S.D. Baalrud, J. Daligault, Effective potential theory for transport coefficients across coupling regimes, Phys. Rev. Lett. 110 (2013) 235001.
[29] J. Daligault, Practical model for the self-diffusion coefficient in Yukawa one-component plasmas, Phys. Rev. E 86 (2012) 047401.
[30] S.D. Baalrud, Transport coefficients in strongly coupled plasmas, Phys. Plasmas 19 (2012) 030701.
[32] F.B. Baimbetov, M.A. Bekenov, T.S. Ramazanov, Effective potential of a semiclassical hydrogen plasma, Phys. Lett. A 197 (1995) 157.
[33] P.K. Shukla, B. Eliasson, Novel attractive force between ions in quantum plasmas, Phys. Rev. Lett. 108 (2012) 165007.
[34] T.S. Ramazanov, K.N. Dzhumagulova, M.T. Gabdullin, Effective potentials for ion-ion and charge-atom interactions of dense semiclassical plasma, Phys. Plasmas 17 (2002) 042703.
[35] Zh.A. Moldabekov, P. Ludwig, M. Bonitz, T.S. Ramazanov, Ion potential in warm dense matter: wake effects due to streaming degenerate electrons, Phys. Rev. E 91 (2015) 023102.
[36] M.H. Thoma, What can we learn from electromagnetic plasmas about the quarkgluon plasma? J. Phys. A Math. Theor. 42 (2009) 214004.
[37] S. Mrowczynski, M.H. Thoma, What do electromagnetic plasmas tell us about the Quark-Gluon plasma? Annu. Rev. Nucl. Part. Sci. 57 (2007) 61.
[38] S.V. Vladimirov, Yu.O. Tyshetzskiy, On description of a collisionless quantum plasma, Phys. Uspekhi 54 (12) (2011) 1243−1256.
[39] P.M. Echenique, F. Flores, R.H. Ritchie, Dynamic screening of ions in condensed matter, Solid State Phys. 43 (1990) 229.
[40] P. Ludwig, W.J. Miloch, H. Kählert, M. Bonitz, On the wake structure in streaming complex plasmas, New J. Phys. 14 (2012) 053016.
[41] Nestro R. Arista, Werner Brandt, Dielectric response of quantum plasmas in thermal equilibrium, Phys. Rev. A 29 (1984) 1471.
[42] C. Deutsch, Nodal expansion in a real matter plasma, Phys. Lett. A 60 (1977) 317. C. Deutsch, Y. Furutani, and M.M. Gombert, Nodal expansions for strongly coupled classical plasmas, Phys. Rep. 69 (1981) 85.
[43] P. Seuferling, J. Vogel, C. Toepffer, Correlations in a two-temperature plasma, Phys. Rev. A 40 (1989) 323.
[44] R. Bredow, Th. Bornath, W.-D. Kraeft, Hypernetted chain calculations for multi-component and nonequilibrium, Contrib. Plasma Phys. 53 (2013) 276.
[45] W. Ebeling, The work of Baimbetov on nonideal plasmas and some recent developments, Contrib. Plasma Phys. 56 (2016) 163.
[46] G. Belyaev, M. Basko, A. Cherkasov, A. Golubev, A. Fertman, et al., Measurement of the Coulomb energy loss by fast protons in a plasma target, Phys. Rev. E 53 (1996) 2701−2707.
[47] C. Deutsch, Gc Maynard, Ion stopping in dense plasmas: a basic physics approach, Matter Radiat. Extrem. 1 (2016) 277−307.
[48] P.E. Grabowski, M.P. Surh, D.F. Richards, F.R. Graziani, M.S. Murillo, Molecular dynamics simulations of classical stopping power, Phys. Rev. Lett. 111 (2013) 215002.
[49] W.D. Kraeft, B. Strege, Energy loss of charged particles moving in a plasma, Phys. A 149 (1988) 313−322.
[51] S. Atzeni, J. Meyer-ter-Vehn, The Physics of Inertial Fusion: Beam Plasma Interaction, Hydrodynamics, Hot Dense Matter, International Series of Monographs on Physics, the Physics of Inertial Fusion, Oxford University Press, Oxford, 2004, 2009.
[52] C. Wang, Y. Long, X.-T. He, J.-F. Wu, W.-H. Ye, et al., Transport properties of dense deuterium-tritium plasmas, Phys. Rev. E 88 (2013) 013106.
[53] S.X. Hu, L.A. Collins, T.R. Boehly, J.D. Kress, V.N. Goncharov, et al., First-principles thermal conductivity of warm-dense deuterium plasmas for inertial confinement fusion applications, Phys. Rev. E 89 (2014) 043105.
[54] J.D. Kress, J.S. Cohen, D.A. Horner, F. Lambert, L.A. Collins, Viscosity and mutual diffusion of deuterium-tritium mixtures in the warm-dense-matter regime, Phys. Rev. E 82 (2010) 036404.
[55] J. Daligault, Liquid-state properties of a one-component plasma, Phys. Rev. Lett. 96 (2006) 065003, 103 (2009) 029901E.
[56] S. Bastea, Viscosity and mutual diffusion in strongly asymmetric binary ionic mixtures, Phys. Rev. E 71 (2005) 056405.
[57] J. Wallenborn, M. Baus, Kinetic theory of the shear viscosity of a strongly coupled classical one-component plasma, Phys. Rev. A 18 (1978) 1737.
[58] L.S. Brown, D.L. Preston, R.L. Singleton Jr., Charged particle motion in a highly ionized plasma, Phys. Rep. 410 (2005) 237.
[59] L. Spitzer, Physics of Fully Ionized Gases, Interscience, N.Y, 1967, p. 586.
[60] D.O. Gericke, M.S. Murillo, M. Schlanges, Dense plasma temperature equilibration in the binary collision approximation, Phys. Rev. E 65 (2002) 036418.
[61] J.N. Glosli, F. Graziani, R.M. More, M.S. Murillo, F.H. Streitz, et al., Molecular dynamics simulations of temperature equilibration in dense hydrogen, Phys. Rev. E 78 (2008) 025401.
[62] Zh.A. Moldabekov, T.S. Ramazanov, M.T. Gabdullin, Equation of state of a dense plasma: analytical results on the basis of quantum pair interaction potentials in the random phase approximation, J. Phys. Conf. Ser. 774 (2016), 012144.
[63] T.S. Ramazanov, Zh.A. Moldabekov, M.T. Gabdullin, Interaction between ions in hot dense plasma via screened Cornell potential, Phys. Plasmas 23 (2016), 042703.
[64] T.S. Ramazanov, S.K. Kodanova, M.K. Issanova, N.K. Bastykova, Zh.A. Moldabekov, The modern information technologies and visualization methods for analysis of computer simulation results for complex plasma, Commun. Comput. Phys. 15 (2014) 981−995.